Proceedings of the Third IASTED International Conference
ADVANCES IN COMPUTER SCIENCE AND TECHNOLOGY
April 2–4, 2007, Phuket, Thailand
ISBN CD: 978-0-88986-656-0

A PC-BASED FREEHAND THREE-DIMENSIONAL ULTRASOUND

Shalihatun Azlin Aziz*, Nor Ashidi Mat Isa*[1], Umi Kalthum Ngah*,
Haidi Ibrahim*, Mohd Ezane Aziz**

*Universiti Sains Malaysia, Engineering Campus,
Seri Ampangan, 14300 Nibong Tebal, Seberang Perai Selatan,
Pulau Pinang, Malaysia.
*[1]Tel: +604 5996051, Fax: +604 5941023, Email: ashidi@eng.usm.my

**Universiti Sains Malaysia, Health Campus,
16150 Kota Bharu, Kelantan, Malaysia.

ABSTRACT
Breast cancer is the number one killer disease among women in Malaysia. In the diagnosis of breast cancer, breast ultrasound examination is commonly used as a supplement to mammography. Ultrasound examination is a non ionizing technique, free of harmful effects. Unfortunately, ultrasound is also known as a time-consuming examination technique with high operator dependency with the results from the examination difficult to discuss, document and reproduce. Three-dimensional imaging provides new information and allows a better interpretation of the standard two-dimensional images. The aim of this study is to therefore develop a PC-based three dimensional ultrasound system to help in the examination and evaluation of breast lesions. The system consists of a PC-based ultrasound system and a magnetic tracking sensor. A sequence of breast ultrasound images were acquired along with the coordinates. These data were then filtered, segmented and finally reconstructed into a 3D image.

KEY WORDS: 3D reconstruction, breast ultrasound, image segmentation.

1. Introduction

Breast ultrasound may be used to view the internal structure of the breast. It is often used in conjunction with mammography to assist in diagnosis during breast screening. Ultrasound can also used to precisely locate the position of a known tumor in order to guide the physician during a biopsy or aspiration procedure[1]. Ultrasound helps to confirm correct needle placement during the procedure [2, 3].

Recently, many studies have been carried out in the three dimensional (3D) segmentation and reconstruction of ultrasound images. This is due to several reasons. One of the main reasons is the limitation of two dimensional (2D) viewing of 3D anatomy using conventional ultrasound. There are areas that do not permit access by normal ultrasound probe [4]. In order to establish diagnosis, the sonographer would have to mentally reconstruct the 3D features of the volume by combining the echographic images together within an approximation of the position of the probe. This practice is inefficient, and may lead to variability and incorrect diagnoses [4, 5]. In addition, a person's imagination varies from one to another, therefore the diagnose for the same case may not be consistent. The 2D ultrasound image represents a thin plane at some arbitrary angle in the body. It is difficult to localize the image plane and reproduce it at a later time for follow-up studies [4]. While linear dimension and cross-sectional area can be determined from a 2D view, the volume, which is the most important clinical parameter, cannot be accurately determined. The current practice frequently in use is mostly based on assumptions regarding the relationship between the observed area and the estimated volume [6].

Image acquired using the imaging modalities like MR and CT are such that the images acquired are regularly spaced. On the other hand, ultrasound acquired images are based on free-hand motion. As of this moment, there are 3 types of approaches for the ultrasound environment. Firstly, using the mechanical probe which is mounted on a motorized guide controller [7]. Secondly, using the transducer array, where a modified freehand probe consists of an imaging plane and a tracking plane [6]. Another technique used is the 3D freehand ultrasound. This technique is based on the acquisition of a set of 2D cross-sectional ultrasound images under the control of the user's hand. What is required is the use of a sensor on the hand-held probe to measure the probe's spatial position and orientation. With such a system, a sonographer moves the sensorized probe over the region of interest, while motion track is measured by the sensor.

As stated above, using 2D ultrasound image from a single slice of the breast tumor might be unable to provide enough information about the tumor. The lack of information could lead to unnecessary action [8]. Using 3D ultrasound, which require slices of ultrasound images containing the whole tumor in order to be reconstruct ensure every angle could be view and display. We believe that 3D ultrasound will overcome this limitation of conventional 2D ultrasound.

In this paper, we attempt to reconstruct a 3D model from a sequence of 2D breast ultrasound images acquired using a freehand probe on a PC-based ultrasound system.

2. Freehand Ultrasound System

A freehand ultrasound system consists of a PC-based ultrasound system (Telemed UltraScan 128 PC-1Z) and a magnetic tracking sensor (miniBird 800, Ascension Technology Corporation). The breast ultrasound images are acquired using a 10 MHz linear array probe. The system is developed with an integrated graphical user interface (GUI) using Borland C++ Builder.

The magnetic tracking sensor consists of a transmitter, a transceiver and a control unit as shown in Fig.1. The control unit then connected to the PC through a RS232 port. A magnetic field is generated by the transmitter while the receiver is mounted on the ultrasound probe. As the probe is moved on the patient, the coordinates can be traced and acquired. The receiver is able to be traced up to 0.8 meter from the transmitter.

Breast ultrasound images are obtained using a PC-based ultrasound system connected to a 10 MHz linear array probe. With the receiver attached to the probe, the coordinates of the probe are obtained. The images with the coordinate of the probe are transmitted to the PC.

After the images and the coordinates of the probe are acquired, the noises typically found on ultrasound images have to be smoothened. The system is unable to reconstruct the 3D image directly from the raw data. This is because the quality of the images is degraded by a special type of acoustic noise known as speckle noise [9, 10]. To reduce this noise, the median filter has been implemented on each ultrasound images. By doing so, the segmentation result for each image can be optimized. Finally, the system projects the segmented images into 3D space and a 3D model is reconstructed.

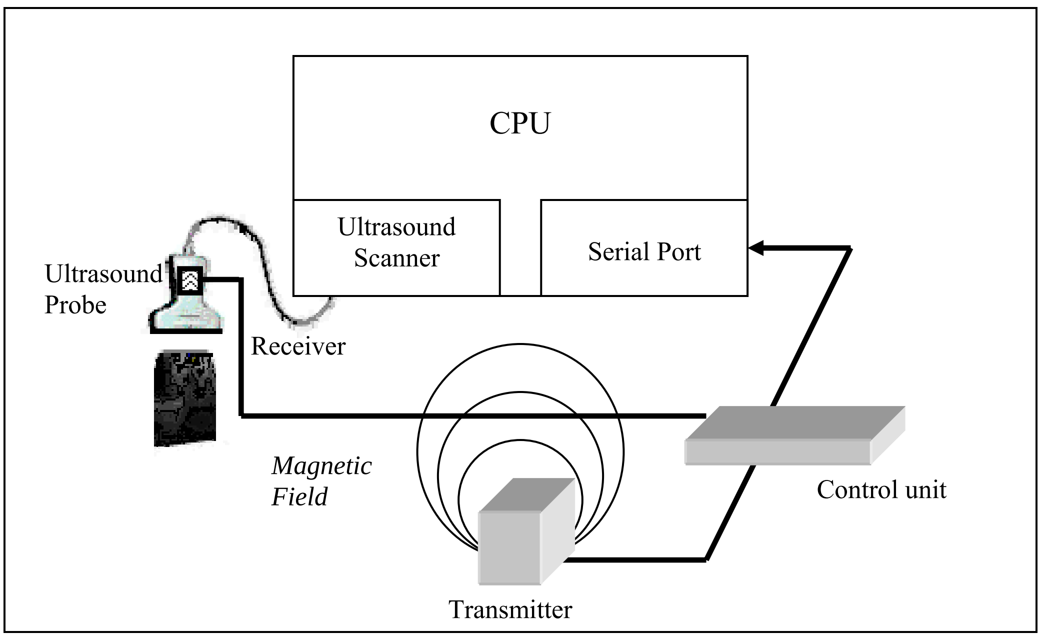

Fig.1. Data acquisition for three-dimensional ultrasound using a freehand scanning system.

2.1 Segmentation

The moving *k*-means clustering technique [11] proposed by Mashor (2000) is a modified version of *k*-means clustering which when applying in positioning the radial basis function (RBF) networks, the moving *k*-means clustering was able to minimise dead centres and centre redundancy problems. Furthermore it is able to reduce the effect of trapped centres in local minima problems [11]. The moving *k*-means clustering algorithm has been proven to produce better segmentation results compared to conventional *k*-means and fuzzy *c*-means clustering algorithms when it was used to segment the medical images [12].

Based on original moving *k*-means clustering algorithm [11], the algorithm of moving *k*-means clustering to be used as segmentation techniques can be implemented as:

1. Initialise the centres and α_0, and set $\alpha_a = \alpha_b = \alpha_0$.
2. Assign all pixels of the image (i.e. in terms of grey level) to the nearest centre and calculate the centre positions using equation:

$$c_j = \frac{1}{n_j} \sum_{i \in c_j} v_i \qquad \ldots(1)$$

3. Check the fitness of each centre using equation:

$$f(c_j) = \sum_{i \in c_j} \left(\left\| v_i - c_j \right\| \right)^2 ; \qquad j = 1,2,\ldots,n_c ;$$
$$i = 1,2,\ldots,N \qquad \ldots(2)$$

4. Find c_s and c_l, the centre that has the smallest and the largest value of *f*(.).
5. If $f(c_s) < \alpha_a f(c_l)$,

   5.1 Assign the members of c_l to c_s if $v_i < c_l$, where $i \in c_l$, and leave the rest of the members to c_l.

   5.2 Recalculate the positions of c_s and c_l according to:

$$\left.\begin{aligned} c_s &= \frac{1}{n_s} \sum_{i \in c_s} v_i \\ c_l &= \frac{1}{n_l} \sum_{i \in c_l} v_i \end{aligned}\right\} \qquad \ldots(3)$$

   Note that c_s will give up its members before step (5.1) and, n_s and n_l in equation (3) are the number of the new members of c_s and c_l respectively, after the reassigning process in step (5.1).

6. Update α_a according to $\alpha_a = \alpha_a - \alpha_a / n_c$ and repeat step (4) and (5) until $f(c_s) \geq \alpha_a f(c_l)$
7. Reassign all pixels to the nearest centre and recalculate the centre positions using equation (1).
8. Update α_a and α_b according to $\alpha_a = \alpha_0$ and $\alpha_b = \alpha_b - \alpha_b / n_c$ respectively, and repeat step (3) to (7) until $f(c_s) \geq \alpha_b f(c_l)$.

where α_0 is a small constant value, $0 < \alpha_0 < \frac{1}{3}$. In this study, the number of cluster is set to two (i.e. each cluster will represent the mass and background regions respectively).

2.2 Voxel-Based Reconstruction

The reconstruction process is done by embedding the acquired images in the image volume. Each pixel is placed at its 3D coordinates (*x, y, z*) in Cartesian grid, according to its 2D image (*x*, y**) and the coordinates obtained from the sensor. Then, for each 3D image point, the voxel value is calculated by interpolation, relatively to its pixel intensity value.

As explained earlier, in this study, the images coordinates are determined with the sensor (receiver) relative to the source (transmitter) in a fixed remote location. Each of the 2D image pixel has coordinates (*x*, y**) relative to the probe, 3D coordinates (*x', y', z'*) relative to the sensor, 3D coordinates (*x", y", z"*) relative to the source and 3D voxel coordinates (*x, y, z*) in the reconstructed image volume.

To render the 3D image in computer graphics, this study used the *homogenous coordinates* [13]. Homogenous coordinates are represented by a four vector (*x, y, z, w*). The conversion between Cartesian and homogenous coordinates was given by:

$$x^* = \frac{x}{w}, y^* = \frac{y}{w}, z^* = \frac{z}{w} \qquad \ldots(4)$$

By setting *w* to zero, the perspective of the view will have an infinite point and any transformation can be applied by using a 4×4 transformation matrix. Hence, the *x*–y** plane would have to be sequentially rotated through the three angles (α, β, γ) about three (given) axes and translated by the vector (*x, y, z*) in order to coincide with the *x'–y'* plane. Therefore, the *x'–y'* plane would similarly have to be rotated through (α', β', γ ') and translated by (*x', y', z'*) in order to coincide with the *x"–y"* plane. Finally, the *x"–y"* plane would have to be rotated through (α", β", γ") and translated by (*x", y", z"*) in order to coincide with the *x–y* plane. Then the embedding transformation from 2D pixel coordinates (*x*, y**) to 3D voxel coordinates (*x, y, z*) can be written as the product of three homogeneous linear transformations, so that:

$$\begin{pmatrix} x \\ y \\ z \\ 1 \end{pmatrix} = T''T'T \begin{pmatrix} x^* \\ y^* \\ 0 \\ 1 \end{pmatrix} \qquad \ldots(5)$$

where, in terms of the 3D rotation matrix

$$R_{ij} = r_{ij}(\alpha, \beta, \gamma) \qquad \ldots(6)$$

$$T = \begin{pmatrix} R_{11} & R_{21} & R_{31} & x \\ R_{21} & R_{22} & R_{23} & y \\ R_{31} & R_{32} & R_{33} & z \\ 0 & 0 & 0 & 1 \end{pmatrix} \qquad ...(7)$$

With similar definitions for T' in terms of

$$R'_{ij} = r_{ij}(\alpha', \beta', \gamma') \qquad ...(8)$$

and T" in terms of

$$R''_{ij} = r_{ij}(\alpha'', \beta'', \gamma'') \qquad ...(9)$$

3. Result

The experiment to visualize the 3D was done on in-vitro results which were acquired using a breast phantom, Breast Ultrasound Needle Biopsy Phantom, Computerized Imaging Reference Systems, Inc).

Fig.2 and Fig.5 show the original data of breast ultrasound images acquired using the ultrasound probe containing two solid masses and one single mass respectively. The data consists of 12 sequential ultrasound images with size 330x250 pixels. Median filter was applied on the images to reduce the noise. Then the filtered images are segmented using the moving *k*-means clustering technique to distinguish between the mass and the normal tissues. The results are shown in Fig. 3 and Fig. 6.

Finally, from the segmented images the data is constructed by the system into a 3D image. The view of the reconstructed 3D images of the mass are shown in Fig.4 and Fig.7 for dataset 1 and 2 respectively.

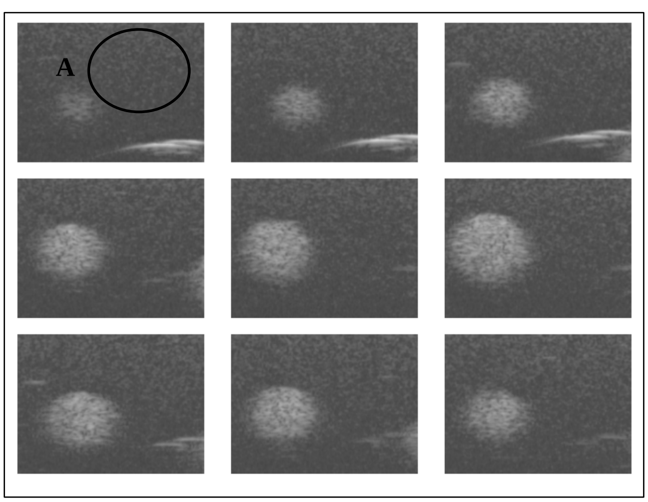

Fig.2. Original data of data set 1 which are acquire using freehand ultrasound probe

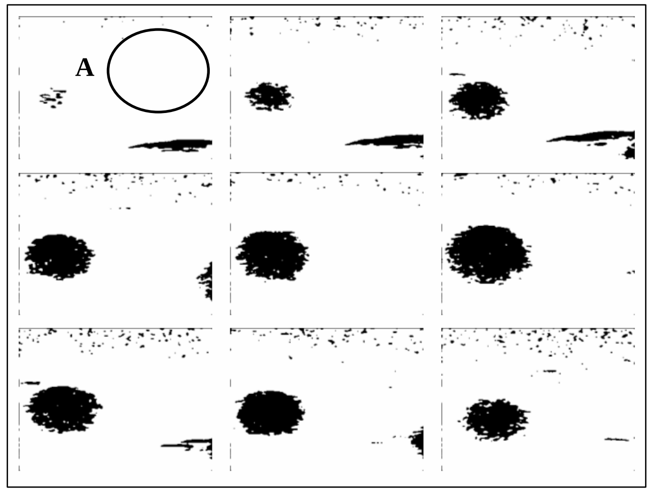

Fig.3. The ultrasound images of dataset 1 after the segmentation using moving *k*-means clustering technique.

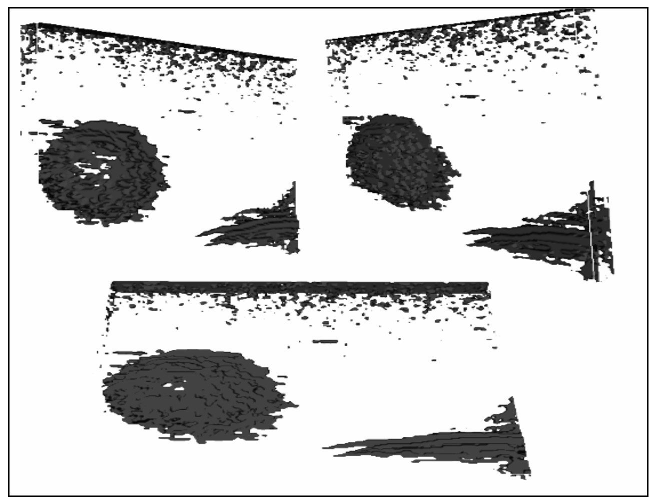

Fig.4. The 3D images of dataset 1 after reconstruction in 3 different views

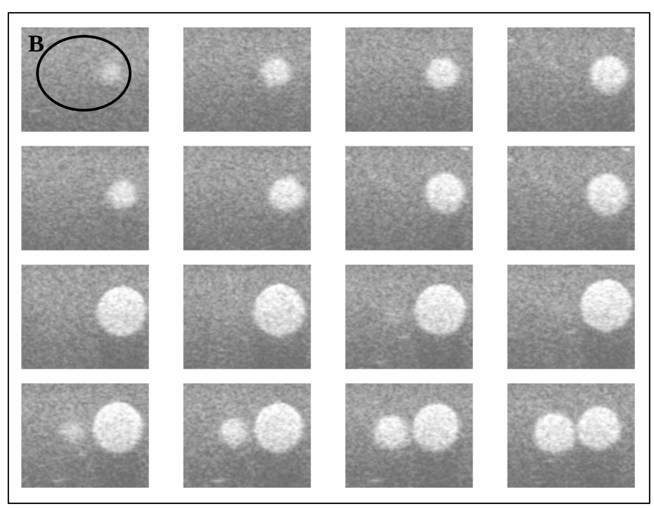

Fig.5. Original data of dataset 2 which are acquire using freehand ultrasound probe

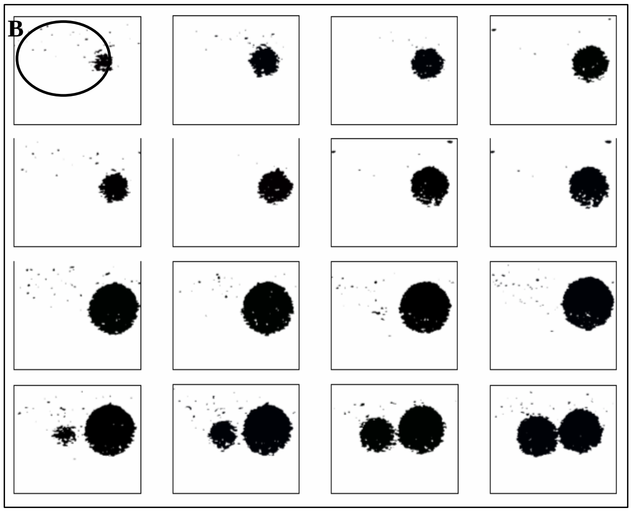

Fig.6. The ultrasound images of dataset 2 after segmentation

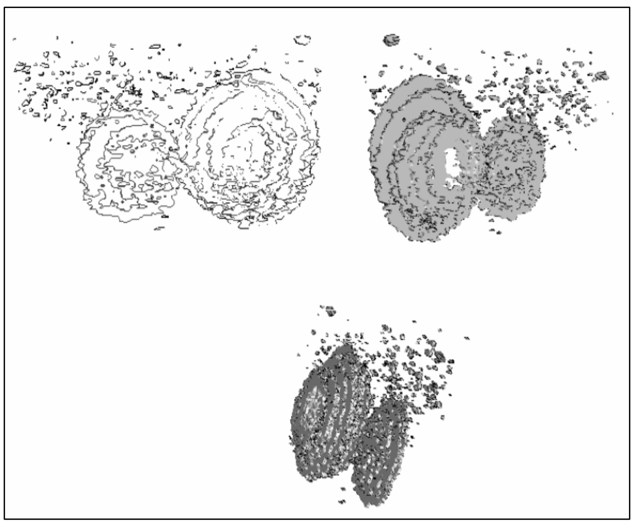

Fig.7. The 3D image after reconstruction from dataset 2 in 3 different views

4. Discussion

In this paper we have presented the results of 3D reconstruction of ultrasound images from a phantom. Two dataset, dataset 1 and dataset 2 has been acquired, enhanced and segmented, finally they were constructed into 3D image.

One of the constraints in order to segment the ultrasound image is the existence of speckle noise. As stated earlier, the speckle noise is a type of acoustic noise that typically exists in ultrasound image. Studies done by [9], [14], [10] and [15] have been focusing on reducing the speckle noise in ultrasound images. Median filter is one of the common method uses in image processing to reduce the speckle noise. Therefore, before segmented the image, median filter has been applied in this study to the images in order to reduce the effect of the speckle noise.

The segmentation technique was used to identify the mass in the ultrasound image. *k*-means clustering technique is often suitable for biomedical image segmentation since the number of clusters (k) is usually known for images of particular regions of human anatomy [16]. Therefore, in this paper, both datasets has been segmented using the modified version of *k*-means called moving *k*-means clustering technique. In doing this, the algorithm has been set into two centres. As shown in Fig.3 and Fig.6, from the images it can be seen that the clustering technique was able to differentiate and classify the images into two classes (i.e. the background and the mass).

Furthermore, the result as shown in Fig.3 and Fig. 6 proved that the combination of median filter and moving *k*-means clustering technique was able to remove most of the speckle noise seen in the original images in Fig.2 and Fig.5 respectively (i.e. speckle noise in Region A for dataset 1 and in region B for dataset 2 have been successfully removed). Unfortunately, the noises can not be remove completely and still appeared in the 3D image. Apart from that, we can see clearly that the edges of the mass are significantly preserved.

From Fig.4 and Fig.7, the results show that apparently, the contours from the 3D image still exist and making the rendering shape unsmooth. This might due to the unsuitable resolution between the images slices and need further investigation.

5. Conclusion

A freehand ultrasound system with the combination of a PC-based ultrasound, a magnetic tracking sensor and image processing technique has been developed. In this paper, two sets of data were acquired using the developed system. Median filtering technique has been applied to enhance the images before segmented the images using moving *k*-means clustering technique. Finally the 3D images were reconstructed.

Certain limitations and difficulties with the rendering technique were encountered and still need to be resolved. The 3D shape was also found to be not smooth. For that, further study will need to be undertaken to overcome the problem. Statistical test should also be performed since in medical domain, apart from precision, robustness is also a very important factor.

References

[1] A. Fenster, K. Surry, W. Smith, J. Gill, D. B. Downey, 3D ultrasound imaging: applications in image-guided therapy and biopsy, *Computers and Graphics* 26, 2002, 557-568.

[2] A. T. Stravros, *Breast Ultrasound* (Lippincott Williams & Wilkins, 2004).

[3] P. Harper, *Ultrasound mammography* (University Park Press, 1989).

[4] O. Oshiro, E. Tanoshima, A. Matani, K. Chihara, 3D Ultrasound Imaging With Echocardiogram and a 3D Positioner. *Proceeding of 19th International Conference-IEEE/EMBS*, 1997

[5] A. Fenster, D. Downey, N. Cardinal, Three-dimensional Ultrasound Imaging. *Phys. Med. Biol.* 46, 2001.

[6] J. A. Hossack, J. S. Ha , T. S. Sumanaweera, Quantitative, Free-Hand 3D Ultrasound Imaging based on a Modified 1D Transducer Array, *Procceeding of SPIE Medical Imaging 2001: Ultrasonic Imaging and Signal Processing*, 4325, 2001, 102-112

[7] Y. Zhang, R. Rohling, D. K. Pai, Direct Surface Extraction from 3D Freehand Ultrasound Images *VIS '02: Proceedings of the conference on Visualization '02,* 2002,45-52.

[8] N. Cho, W.K. Moon, J.H. Cha, S M. Kim, B.K. Han, E.K. Kim, M.H. Kim, S.Y. Chung, H.Y. Choi, J.G. Im, Differentiating Benign from Malignant Solid Breast Masses: Comparison of Two-Dimensional and Three Dimensional US. *Radiology* 240, 2006, 26-32.

[9] C. Chinrungrueng, A. Suvichakorn, Fast Edge-preserving Noise Reduction for Ultrasound Images, *IEEE Transactions On Nuclear Science*, 48(3), 2001.

[10] R. N. Czerwinski, D. L. Jones, W. D. O'Brien Jr., Edge Detection in Ultrasound Speckle Noise, *Image Processing, 1994. Proceedings. ICIP-94., IEEE International Conference.* 3, 1994.

[11] M. Y. Mashor, Hybrid Training Algorithm for RBF Network *International Journal of the Computer, The Internet and Management,* 8(2), 2000, 50-65.

[12] N. A. Mat Isa, M. Y. Mashor, N. H. Othman, Comparison of Segmentation Performance of Clustering Algorithms for Pap Smear Images, *Proceeding of the International Conference on Robotics, Vision, Information and Signal Processing,* 2003, 118-125.

[13] W. Schroeder, K. Martin, B. Lorensen, *Visualization Toolkit: An Object-Oriented Approach to 3D Graphics.* (Prentice Hall, 1998).

[14] J. Hu, X. Hu, Applications of Median Filter to Speckle Suppression in Intravascular Ultrasound Images, *Proceedings of the 1994 Intelligent Information Systems,* 1994, 302-306.

[15] R. N. Czerwinski, D. L. Jones,Detection of Lines and Boundaries in Speckle Images - Application to Medical Ultrasound, *IEEE Transactions on Medical Imaging,*18(2),1999, 126-136.

[16] C. W. Chen, J. Luo, K. J. Parker, Image Segmentation via Adaptive K-Mean Clustering and Knowledge-Based Morphological Operations with Biomedical Applications, *IEEE Transactions on Image Processing,* 7(12), 1998 1673-1683.